ISBN: 978-3-95450-231-8 ISSN: 2673-5490 doi: 10.18429/JACoW-IPAC2023-WEPA025

SPACE-CHARGE LIMIT IN HADRON SYNCHROTRONS INDUCED BY A GRADIENT ERROR

Dmitrii Rabusov*, Diamond Light Source, Oxfordshire, UK
Adrian Oeftiger†, GSI Helmholtzzentrum für Schwerionenforschung GmbH, Darmstadt, Germany

Abstract

The half-integer resonance is considered to be one of the strongest effects limiting the intensity of the FAIR SIS100 heavy-ion synchrotron which is currently under construction at GSI. Results of simulations under realistic synchrotron-operation conditions show that for bunched beams, a relatively small gradient error can result in a large half-integer stop-band width significantly reducing the maximum achievable bunch intensity. In addition to the results of simulations in SIS100, we characterize the half-integer stop band in SIS18 using experimental data.

SPACE-CHARGE LIMIT IN SIS100

The aim of this work is to identify the space-charge limit due to the half-integer stop band (when the bare tune $Q = n/2$, n is integer), also known as the maximum tolerable space-charge tune shift, for realistic Gaussian-like distributed bunched beams and realistic time scales for hadron synchrotrons. SIS100 is expected to operate at the space-charge limit [1] in the vertical plane. We use the vertical plane in this study to avoid dispersion-related effects. Detailed overview of the results can be found in Refs. [2, 3].

Theoretical Background

The stop-band width at negligible intensity [4] amounts to the integral, $F_n = \frac{1}{2\pi} \oint \beta(s)\, \Delta k(s)\, \exp\left(-i n \frac{2\pi\, \mu(s)}{Q}\right) \mathrm{d}s$ over the path length s, where $\beta(s)$ and $\mu(s)$ are the optical Twiss and phase advance functions, $\Delta k(s)$ are gradient errors, $n = 37$ (for SIS100). In this work, F_n is used as the gradient-error strength. A conceptual way to estimate the strength of space charge is to calculate

$$\Delta Q^y_{\mathrm{KV}} = -\frac{K_{\mathrm{sc}}\, R^2}{4\, \langle \sigma_y \rangle\, (\langle \sigma_x \rangle + \langle \sigma_y \rangle)\, Q_y}\,, \qquad (1)$$

which is the KV [5] tune shift where $K_{\mathrm{sc}} = \frac{Z e I}{2\pi\, \epsilon_0\, m_0\, (\gamma_r\, \beta_r\, c)^3}$ (space-charge perveance), averaging $\langle \cdot \rangle$ over s, the effective ring radius is R, the beam peak current I, the ion charge number Z, the proton elementary charge e, the vacuum permittivity ϵ_0, the rest mass of the ions m_0, the speed of light c, and relativistic factors γ_r, β_r. In the case of coasting KV beams with negligible coupling and no dispersion effects, the location of the half integer resonance is determined by

$$2\,Q - \Delta Q_{\mathrm{env}} = n\,, \qquad (2)$$

where n in an integer number, ΔQ_{env} is the envelope tune shift [6] which amounts to $2\,C\,\Delta Q_{\mathrm{KV}}$, and C is the transverse geometry factor ($C = 2/3$ in the case of SIS100).

* dmitrii.rabusov@diamond.ac.uk
† a.oeftiger@gsi.de

Simulation Model

This work shows the results obtained with a simulation model where element-by-element particle tracking through the SIS100 lattice with gradient errors is provided by SixTrackLib [7]. The direct space-charge interaction of a bunched Gaussian-like beam is computed using the 2.5D particle-in-cell (PIC) solver with the PyHEADTAIL [8] tracking code. The setup includes 64 longitudinal bunch slices and 128×128 grid. We use 10^6 macro particles with 10^3 space charge nodes equidistantly located in the accelerator lattice.

As an example of the results provided by the simulation model, we show emittance-growth curves for various values of the synchrotron tune Q_s at the vertical bare tune $Q_y = 18.62$ (slightly above the linear resonance condition, Eq. 2) corresponding to the strong-gradient error scenario (see Table 1). In this work, we set $Q_x = 18.95$ to avoid the Montague resonance [9] for all probed ΔQ_{env}. The red, blue, and orange lines correspond to increasing values of Q_s. During the first 50 turns, the vertical emittance increases linearly, and the increase is equivalent for any Q_s. After this, the speed of the linear growth is reduced but no saturation observed. The total emittance growth for a given turn at later times increases with increasing synchrotron tune Q_s.

Table 1: Reference values of the stop-band integral.

	Weak	Intermediate	Strong
$\lvert F_{37} \rvert$	$0.6 \cdot 10^{-3}$	$2.6 \cdot 10^{-3}$	$4.3 \cdot 10^{-3}$

Throughout this work we use a threshold level of $\frac{1}{\epsilon_0}\frac{d\epsilon}{dn} = 5 \cdot 10^{-6}$. Any working point with emittance growth above this threshold is considered as affected by the resonance. This amounts to an overall emittance growth of 0.5% and

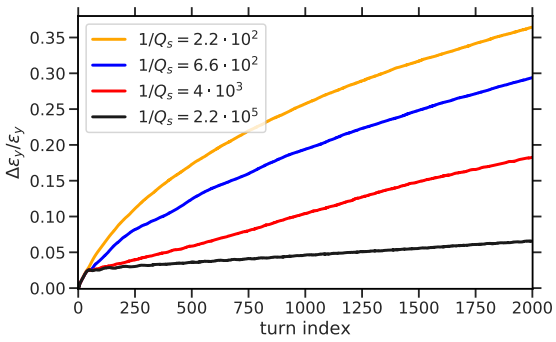

Figure 1: Vertical emittance growth vs. the synchrotron tune.

ISBN: 978-3-95450-231-8 ISSN: 2673-5490 doi: 10.18429/JACoW-IPAC2023-WEPA025

80% during 10^3 turns and the injection plateau of SIS100 (around one second) correspondingly.

Maximum Tolerable Intensity

The classical conceptual discussion of the space-charge limit relates to the linear resonance condition [10, 11] which is valid in the case of coasting beams. For a finite gradient error, the space-charge limit (the maximum achievable intensity) is reached when $\Delta Q_{\mathrm{env}} < 1$. This condition does not depend on the strength of the gradient error.

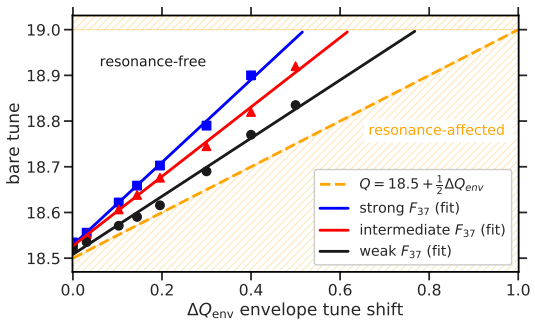

Figure 2: Space-charge limit.

For bunched beams, any working point between the half-integer bare tune and the linear resonance condition is affected by the resonance. Figure 2 depicts this concept, the orange dashed line corresponds to the linear resonance condition, and the area below it is "forbidden". Furthermore, in the case of bunched beams, the half-integer stop band extends to above the linear resonance condition which might lead to unacceptable particle losses for time scales relevant to SIS100. Working points inside the stop band are not expected to conserve RMS emittances of bunched beams at non-zero space charge, finite synchrotron motion, and a finite gradient error (see Fig. 1 and Ref. [2]). Black dots, red triangles, and blue squares in Fig. 2 correspond to the upper edge of the half-integer stop band for weak, intermediate, and strong gradient-error scenarios. Compared to the conceptual discussion on the space-charge limit, simulation results show that a finite gradient error leads to a steeper inclination of the upper-edge curves (colored solid lines) than the linear resonance condition. Effectively, the space-charge limit in simulations is reached when the upper edge intersects with the next half-integer bare tune. This corresponds to the scenario where adjacent half-integer stop bands occupy the entire (Q_x, Q_y) diagram.

Classical conceptual space-charge limit in SIS100 is predicted to be $\Delta Q_{\mathrm{env}} = 1$, regardless of the gradient-error strength. On the other hand, linear extrapolation of the simulation results including a certain gradient error indicates a maximum achievable intensity (in terms of ΔQ_{env}). The scenario of strong gradient error results in a limit of only $\Delta Q_{\mathrm{env}} \simeq 0.5$, the intermediate gradient error in $\Delta Q_{\mathrm{env}} \simeq 0.6$, and the weak gradient error in $\Delta Q_{\mathrm{env}} \simeq 0.8$.

To conclude, we find that, for realistic Gaussian-distributed bunched beams, a relatively small stop-band width at zero space charge ($\simeq 10^{-3}$, see Table 1) can result in a significant reduction of the maximum intensity (here by a factor 2 for the strong gradient-error scenario). As a consequence, control and compensation of gradient errors are crucial for a synchrotron to maintain the highest intensities under strong space-charge conditions.

EXPERIMENT IN SIS18

This section presents two approaches for characterizing the half-integer stop band in the SIS18 heavy-ion synchrotron at GSI. To compensate for gradient errors across the ring, a pair of quadrupole corrector magnets can be utilized. In this study, the horizontal bare tune was set to $Q_x = 4.32$, and the vertical bare tune was set above $Q_y = 3.5$ to examine the $7/2$ half-integer resonance. A quadrupole corrector loop configuration was utilized with both correctors powered at the same strength but with opposite signs, and the beta function design was identical in both locations. Consequently, the bare tunes of SIS18 remained constant for any corrector loop strength, while the stop-band integral at zero intensity, denoted as F_7, changed. The experiment used a $^{40}\mathrm{Ar}^{10+}$ bunched beam with an energy corresponding to 8.6 MeV/u (the nominal injection energy was 11.4 MeV/u, reduced during the experiment via UNILAC), a revolution frequency of 186.04 kHz, and a chromaticity of zero via sextupole magnets. The intensity varied in the range of $3 \cdot 10^9 \leq \mathrm{N} \leq 1.2 \cdot 10^{10}$, with an RMS of $(\epsilon_x, \epsilon_y) = (13.5, 6.1)$ mm mrad. Further experimental details can be found in Ref [3].

Upper Edge from Particle Losses

The first approach is a dynamic tune scan similar to Ref. [12]. The upper edge of the half-integer stop band is identified during a single SIS18 cycle. The vertical bare tune descends toward $7/2$ during $\simeq 0.1$ s keeping all other machine parameters constant. The red curve in Fig. 3 (left) corresponds to the variation of Q_y. Vertical lines (blue dashed, black dotted, and orange dot-dash) indicate the timings of the SIS18 cycle: injection from UNILAC to SIS18, the start of the Q_y descent, and the tune return correspondingly. When the vertical bare tune intersects the half-integer stop band, particle losses occur. This effect can be measured using a Direct-Current Current Transformer (DCCT) as shown in Fig. 3 (right). In order to accurately determine the location of the upper edge, the loss rate $\frac{1}{N}\frac{\mathrm{d}N}{\mathrm{d}t}$ can be used, where the

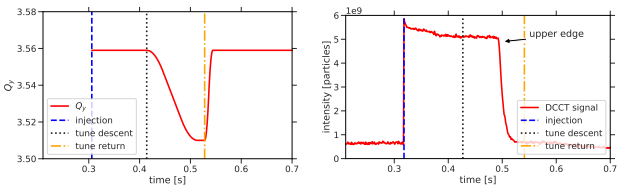

Figure 3: SIS18 dynamic-scan cycle (left) and the beam intensity during it (red curve, right).

ISBN: 978-3-95450-231-8 ISSN: 2673-5490 doi: 10.18429/JACoW-IPAC2023-WEPA025

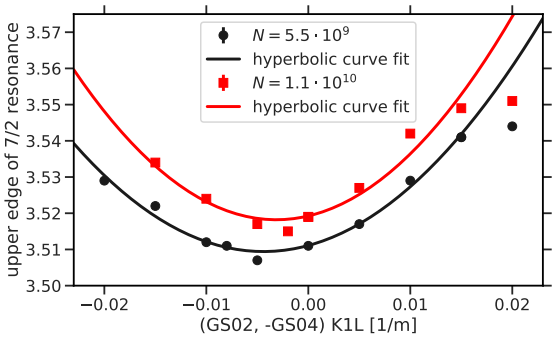

Figure 4: Half-integer stop-band minimization in SIS18.

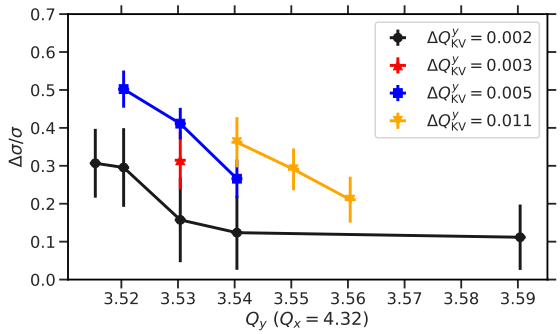

Figure 6: Results of beam size measurements, the strength of the corrector loop is zero.

change of the number of particles N is normalized by the maximum amount of particles (after the injection).

Figure 4 displays the location of the upper edge of the half-integer stop band against the strength of the corrector loop for two probed intensities (both corresponding to $\Delta Q^y_{\mathrm{KV}} \simeq 0.01$), denoted by black dots and red squares, the error bars indicate the precision of the bare-tune measurements (without a systematic error). The minimum distance between the upper edge and the half-integer occurs when SIS18 is in its optimal configuration. To determine the optimal value of the corrector-loop strength, interpolation by the upper branch of the hyperbola is performed, and both curves show a similar behavior. Though the reduction of the stop band (at $\Delta Q^y_{\mathrm{KV}} \simeq 0.01$) is only ≤ 0.01, this correction can play a supporting role to achieve the high FAIR intensities. The upper edge is systematically higher in the case of the red curve due to additional particle losses associated with measured initial larger transverse beam sizes.

Upper Edge from Beam-Size Measurements

The second experimental setup, a static tune scan, is used to isolate the effects that lead to particle losses. In this setup, the change of Q_y (shown in Fig. 5 with the red curve on the left) lasts only $\simeq 0.016$ s. Next, it stays at a lower point on a so-called "tune plateau" for $\simeq 0.1$ s (here, the probed tune $Q_y = 3.51$). Finally, Q_y returns to the initial location. Unlike the dynamic tune scan, this approach requires several SIS18 cycles for probing different values of the vertical bare tune. This is necessary to ensure the same space-charge conditions for all probed values of Q_y. In this setup, the growth of the vertical beam size at a probed Q_y is measured using the Ionization Profile Monitor (IPM) [13]. The example of the beam size measurements during the static tune scan is illustrated in Fig. 5 on the right. Black dots and red squares represent the IPM output before and after the tune plateau correspondingly. Transverse profiles are fitted with Gaussian distribution taking the change of the bunch intensity into account. To eliminate the influence of lattice functions we define vertical beam-size growth as $\Delta\sigma/\sigma = (\sigma_0 - \sigma_1)/\sigma_0$, where σ_0 is measured before the tune descent, and σ_1 after the tune ascent. Figure 6 demonstrates the response of the vertical beam-size growth to the vertical bare tune Q_y for various values of space charge (due to an upstream intensity variation in UNILAC). Black dots, red upward triangles, blue squares, and orange downward triangles correspond to the values of vertical beam-size growth $\Delta\sigma/\sigma$ obtained with increasing space charge. However, more data points for different Q_y (for all probed intensities) are required to acquire a desirable resolution for the upper-edge identification.

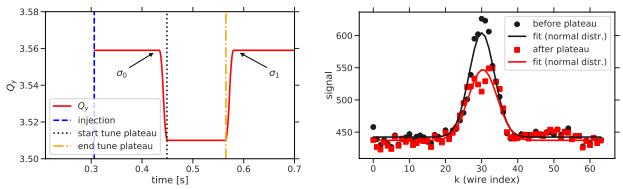

Figure 5: SIS18 static-scan cycle and vertical beam profiles during it (right).

CONCLUSIONS

The simulation study for Gaussian bunches over long-term time scales (several synchrotron oscillation periods) resulted in a key insight of practical relevance to existing and future synchrotrons. Even a relatively small gradient error (resulting in a zero-space-charge stop-band width of just $\simeq 10^{-3}$) can considerably reduce the maximally achievable bunch intensity (in the SIS100 example by a factor $\simeq 2$). We note that this effect, whilst absent in classical discussions of the space-charge limit, must be taken into account under realistic synchrotron operation conditions (bunched beam, long storage time). Two approaches are proposed for the experimental verification of the scheme for the half-integer stop-band characterization in SIS18 for separate applications: The dynamic scan for optimization (time-efficient), the static scan for the space-charge-limit estimations (accurate).

REFERENCES

[1] A. Oeftiger, O. Boine-Frankenheim, V. Chetvertkova, V. Kornilov, D. Rabusov, and S. Sorge, "Simulation study of the space charge limit in heavy-ion synchrotrons," *Phys. Rev. Accel. Beams*, vol. 25, p. 054 402, 5 2022. doi:10.1103/PhysRevAccelBeams.25.054402

ISBN: 978-3-95450-231-8 ISSN: 2673-5490 doi: 10.18429/JACoW-IPAC2023-WEPA025

[2] D. Rabusov, A. Oeftiger, and O. Boine-Frankenheim, "Characterization and minimization of the half-integer stop band with space charge in a hadron synchrotron," *Nucl. Instrum. Methods Phys. Res., Sect. A*, vol. 1040, p. 167 290, 2022. doi:10.1016/j.nima.2022.167290

[3] D. Rabusov, "Characterization and minimization of the half-integer stop band with space charge in hadron synchrotrons," en, Ph.D. dissertation, Technische Universität Darmstadt, 2023, VIII, 112 Seiten. doi:10.26083/tuprints-00023222

[4] S. Y. Lee, *Accelerator Physics*. WORLD SCIENTIFIC, 2011. doi:10.1142/8335

[5] I. M. Kapchinskij and V. V. Vladimirskij, "Limitations Of Proton Beam Current In A Strong Focusing Linear Accelerator Associated With The Beam Space Charge," in *2nd International Conference on High-Energy Accelerators*, 1959, pp. 274–287.

[6] F. J. Sacherer, "Transverse space charge effects in circular accelerators," Presented 30 Oct 1968, Ph.D. dissertation, University of California, Berkeley, 1968. doi:10.2172/877342

[7] M. Schwinzerl, R. De Maria, K. Paraschou, H. Bartosik, G. Iadarola, and A. Oeftiger, "Optimising and Extending a Single-particle Tracking Library for High Parallel Performance," in *Proceedings of the 12th International Particle Accelerator Conference*, 2021, THPAB190. doi:10.18429/JACoW-IPAC2021-THPAB190

[8] A. Oeftiger, "An Overview of PyHEADTAIL," CERN, Tech. Rep. CERN-ACC-NOTE-2019-0013, 2019. https://cds.cern.ch/record/2672381

[9] B. W. S. L. Montague, "Fourth-order coupling resonance excited by space-charge forces in a synchrotron," CERN, Tech. Rep. CERN-1968-038, 1968. doi:10.5170/CERN-1968-038

[10] A. Fedotov and I. Hofmann, "Half-integer resonance crossing in high-intensity rings," *Physical Review Special Topics-Accelerators and Beams*, vol. 5, no. 2, p. 024 202, 2002. doi:10.1103/PhysRevSTAB.5.024202

[11] R. Baartman, "Betatron resonances with space charge," *AIP Conf. Proc.*, vol. 448, no. 1, pp. 56–72, 1998. doi:10.1063/1.56781

[12] T. Uesugi, S. Machida, and Y. Mori, "Experimental study of a half-integer resonance with space-charge effects in a synchrotron," *Phys. Rev. ST Accel. Beams*, vol. 5, p. 044 201, 4 2002. doi:10.1103/PhysRevSTAB.5.044201

[13] P. Forck, A. B. Bank, T. Giacomini, and A. Peters, "Profile Monitors Based on Residual Gas Interaction," in *Proc. DIPAC'05*, Lyon, France, Jun. 2005. https://jacow.org/d05/papers/ITTA01.pdf